



METHODOLOGY

Open Access

Dual patch voltage clamp study of low membrane resistance astrocytes *in situ*

Baofeng Ma¹, Guangjin Xu², Wei Wang¹, John J Enyeart¹ and Min Zhou^{1*}

Abstract

Whole-cell patch clamp recording has been successfully used in identifying the voltage-dependent gating and conductance properties of ion channels in a variety of cells. However, this powerful technique is of limited value in studying low membrane resistance cells, such as astrocytes *in situ*, because of the inability to control or accurately measure the real amplitude of command voltages. To facilitate the study of ionic conductances of astrocytes, we have developed a dual patch recording method which permits membrane current and membrane potential to be simultaneously recorded from astrocytes in spite of their extraordinarily low membrane resistance. The utility of this technique is demonstrated by measuring the voltage-dependent activation of the inwardly rectifying K⁺ current abundantly expressed in astrocytes and multiple ionic events associated with astrocytic GABA_A receptor activation. This protocol can be performed routinely in the study of astrocytes. This method will be valuable for identifying and characterizing the individual ion channels that orchestrate the electrical activity of low membrane resistance cells.

Keywords: Astrocytes, Voltage clamp, Membrane resistance, Kir4.1, GABA_A receptor

Introduction

When patch clamp was first applied to study glial cells in brain slices in the early 1990s, it became immediately clear that in a subpopulation of glial cells, characterized by a linear current-to-voltage (*I-V*) relationship passive K⁺ membrane conductance and low membrane resistance (R_M), adequate voltage clamp quality could not be achieved [1,2]. In later studies, this subpopulation of glial cells has been unequivocally shown as the only electrophysiological phenotype of astrocytes in rat hippocampus when animals reach adulthood [3,4]. Therefore, the expression of passive membrane K⁺ conductance is a characteristic of functional mature astrocytes. In view of a widespread distribution of passive astrocytes in various brain regions and in species ranging from low amphibians to humans, it is possible that the distinctive passive K⁺ conductance and low R_M are common features of mature astrocytes in the brain.

Despite of an increasing awareness of the functional importance of astrocytes in the brain, the exceptionally low R_M , estimated in the range of 2–5 MΩ, creates a

formidable barrier for patch clamp voltage study of this major glial type. Specifically, the low R_M introduces a large error because a significant fraction of the voltage drop during a command potential occurs across the electrode tip rather than the cell membrane [5]. Because of this limitation, it has been difficult to identify and characterize the ion channels and transporter activities that establish the electrical properties of astrocytes. In particular, astrocytes are known to express a variety of K⁺ channels, including inwardly rectifying Kir4.1 and two-pore domain (K2P) TWIK-1 and TREK-1 leak-type K⁺ channels. The inability to effectively voltage clamp astrocytes has prevented these currents from being individually characterized with respect to their relative functional expression, conductance, rectification, contribution to V_M , and modulation by neurotransmitters through activation of G-protein-coupled receptors. Therefore, an alternative electrophysiological method is urgently needed, and if such a new method could be successfully developed, voltage clamp study would be invaluable to gain insights into the basic electrophysiological properties of astrocytes in the adult brain.

* Correspondence: zhou.787@osu.edu

¹Department of Neuroscience, The Ohio State University Wexner Medical Center, Columbus, OH 43210, USA

Full list of author information is available at the end of the article

Rationale and validation of dual patch single cell recording technique

To circumvent the limitation imposed by conventional whole-cell patch clamp recording for study of low R_M astrocytes, we have developed a dual patch voltage clamp method. In this method, two patch electrodes are sealed to the cell body of a single astrocyte in the whole-cell configuration. This design has been conceived to overcome the following limitations inherited by single electrode voltage patch clamp for study of low R_M cells. In single electrode patch clamp recording, the R_M is typically calculated from the fit of a voltage command (V_C) induced membrane current (I) near the resting membrane potential that carries a large error in low membrane resistance cells (see details in the following sections). In contrast, in dual patch recording, the V_C is applied through one patch electrode, while a second electrode is used to measure the V_C -induced actual change in membrane potential (V_M). Using this method, an accurate current-to-voltage (I - V_M) relationship can be obtained over a wide range of potentials, and the voltage-dependent membrane conductance can be reliably calculated. An additional unique opportunity offered by dual patch recording is that the I , V_M , and R_M can be measured and calculated simultaneously. This, however, needs to be experimentally validated.

In the present study, we started with a direct measurement of voltage errors in low R_M astrocytes with dual

patch recording. That was followed by the validation of dual patch recording for reliable and accurate measurement of R_M . Building upon these, we further showed that the voltage dependent activation kinetics of inwardly rectifying K^+ channel conductance can be established and pharmacologically studied. Finally, astrocytic ionotropic GABA_A receptor was used as an example to show the simultaneous measurement of I , V_M , and R_M and disclosure of multiple ionic events associated with astrocytic GABA_A receptor activation.

A lack of voltage control in astrocyte recording in situ

Astrocytes were identified for recording based on cell soma morphology and SR101 staining in the CA1 *stratum radiatum* (Figure 1a). Consistent with our previous report, functional mature hippocampal astrocytes after postnatal day 21 identically express a linear current-to-voltage (I - V) relationship membrane K^+ conductance, or passive K^+ conductance (Figure 1b) [3]. To directly assess the voltage clamp quality, a MultiClamp 700B amplifier designed for dual channel recording was used. Two patch electrodes were sealed sequentially on a single astrocyte. Electrode one (E1) and two (E2) were maintained in voltage clamp and current clamp mode, respectively (Figure 1a). The same recording configuration was also used for NG2 glia for comparison of voltage clamp quality. NG2 glia are morphologically similar to astrocytes in terms of the soma

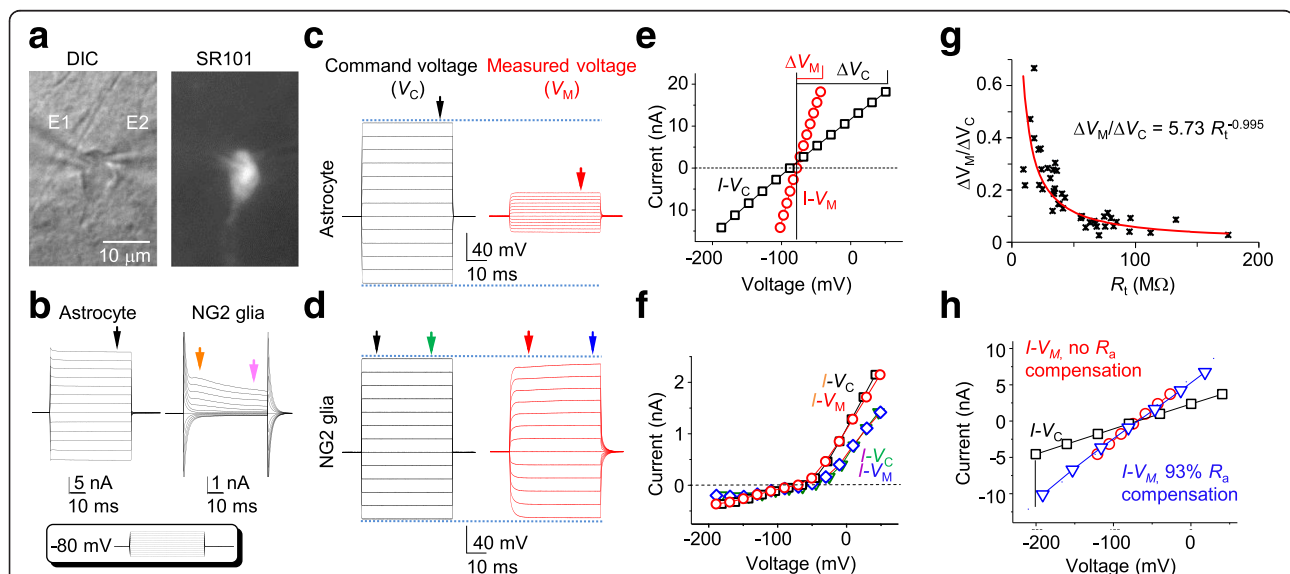


Figure 1 Poor voltage clamp quality in astrocyte recording. (a) DIC and SR101 fluorescent images of a dual patch recorded astrocyte in the hippocampal CA1 *stratum radiatum* region; electrode 1 (E1) and electrode 2 (E2) were in voltage clamp and current clamp modes, respectively. (b) Whole-cell current profiles of an astrocyte and an NG2 glia are shown as indicated; the cells were held at resting (-80 mV), then stepped to command voltages from -180 mV to $+20$ mV with 20 mV increments (inset). (c, d) Comparison of command voltages (V_C) applied through E1 and the resultant potentials across the membrane (V_M) measured from E2 for the recorded astrocyte and NG2 glia, respectively. (e, f) The I - V_C and I - V_M were plotted in the same chart for voltage clamp quality comparison. (g) The R_t was plotted against $V_M/\Delta V_C$ ($n = 44$) and fitted with $\Delta V_M/\Delta V_C = aR_t^b$; the $V_M/\Delta V_C$ decreases with increasing R_t , which yields R_M and exponent values of 5.73 $M\Omega$ and -0.995 , respectively. (h) Comparison of I - V_M relationships in the presence and absence of R_a compensation, showing a good voltage clamp quality after R_a compensation.

shape *in situ*, but can be identified based on the absence of SR101 staining and expression of voltage-gated K⁺ channel conductances. In both cases, the V_C was applied through E1, which induced a characteristic passive K⁺ conductance in the low R_M astrocyte, and outward voltage-gated transient and delayed rectifier K⁺ channel currents in the high R_M NG2 glia (Figure 1b). In E2, the V_C -induced actual V_M was recorded simultaneously (Figure 1c, d). Both $I-V_C$ and $I-V_M$ were plotted for comparison of voltage clamp quality (Figure 1e, f), where the V_M was only $19.0 \pm 1.7\%$ of the V_C in astrocytes ($n = 54$), in contrast, $I-V$ curves in NG2 glia were nearly superimposable. The plots shown in Figure 1e, f further display a striking difference in the voltage clamp quality between these two glial subtypes.

Since the total membrane resistance (R_t) is the sum of access resistance (R_a) and membrane resistance (R_M) in series [6], to confirm that the dual patch results obey the basic voltage-division principle as in single electrode patch clamp recording, we used $\Delta V_M/\Delta V_C$ as an indicator of voltage clamp quality that theoretically follows a relationship of $\Delta V_M/\Delta V_C = R_M R_t^{-1}$. We plotted R_t against $\Delta V_M/\Delta V_C$ and fit the data with $\Delta V_M/\Delta V_C = a R_t^b$ from 44 dual patch recordings (Figure 1g). Of note, to obtain an accurate fit, the R_t greater than 30 M Ω that are routinely discarded in study were included in this analysis. As shown in the Figure 1g, the fit yielded a R_M (a) of 5.73 M Ω that was almost identical to the measured R_M (see next section). Importantly, the fit yielded an exponent (b) of -0.995 , which matches closely to a theoretically ideal value of -1 , indicating that the results derived from the two electrodes in dual patch recording follow accurately to the voltage-division principle.

In dual patch recording, E1 and E2 are separated by $3.4 \pm 0.2 \mu\text{m}$ ($n = 15$), and the V_M measured from E2 ($V_{M,2}$) is used to represent the V_M in E1 ($V_{M,1}$) to establish the actual $I-V_M$ relationship, therefore to what extent does $V_{M,2}$ reflect the intended $V_{M,1}$ is an issue to be resolved for the concern of space clamp error, especially for low R_M astrocytes. To estimate $V_{M,1}$ in E1, we assumed that R_a is 1.5-fold of the recording electrode resistance (R_p) and used a $-40 \text{ mV } V_C$ to induce current (I). Subsequently, the $V_{M,1}$ is calculated from $(V_C - 1.5 R_p * I)/I$, and the fidelity of $V_{M,2}$ in the form of $V_{M,2}/V_{M,1}$ is estimated at 93.9% ($n = 4$). Thus, within a tip-to-tip distance < than 4 μm in our study, $V_{M,2}$ can be used with high fidelity for $I-V_M$ plot and for the R_M measurement that will be described in the following section.

NG2 glia typically exhibits a R_M greater than 200 M Ω [7], or a R_a/R_t ratio of $\sim 1/20$; therefore, greater than 95% of the V_C is distributed across R_M , permitting good voltage clamp study (Figure 1d) as compared to the poor clamp quality in astrocytes. To determine the extent to which R_a compensation could be useful for improving the voltage clamp quality in low R_M astrocyte, we first

used E2 as a voltage monitor in dual patch recording to guide the adjustment of R_a , C_M and prediction/correction parameters in E1. Occasionally, it was possible to achieve a nearly perfect voltage control (Figure 1h). However, without E2 as a voltage referee, conventional empiric guided R_a compensation resulted in a largely variable range of voltages, specifically, the voltage improvement varied from 40% to 143% from 27 trials in 3 cells. Additionally, the R_a typically varies significantly during the recording (see Figure 2f), thus, it was impossible to use a preset R_a compensation parameters in the entire course of recording. Therefore, R_a compensation is not practically useful for clamp quality improvement in low R_M astrocyte.

R_M can be accurately measured in dual patch single cell recording

The low R_M of passive astrocytes is the cause of poor voltage clamp quality. In dual patch recording, the V_C -induced I and the actual voltage drop across the membrane V_M , are measured separately by the two electrodes, so that R_M can be calculated accurately from $R_M = V_M/I$. Using dual patch recording, the voltage and current clamp modes can be alternated between E1 and E2 (Figure 2a), allowing R_M and R_a to be measured for each electrode from the same cell. We therefore analyzed these results to determine 1) whether R_{M1} and R_{M2} are identical in the same cell, as expected, and 2) whether the R_M in dual patch recording is truly independent of the variation of R_a . We used the difference in measured access resistances ($R_{a1}-R_{a2}$) and membrane resistances ($R_{M1}-R_{M2}$) to determine the variation of these two parameters in the same cell. The results showed that, in the same cell, the R_a varied considerably between E1 and E2 (Figure 2b, red open circles), while the R_{M1} and R_{M2} were essentially identical (Figure 2b, black open circles). We next compared the measured R_M values from E1 and E2 and found that these were nearly identical (R_{M1} , $6.00 \pm 0.32 \text{ M}\Omega$ vs. R_{M2} , $6.12 \pm 0.33 \text{ M}\Omega$, $n = 54$, $P = 0.79$). Finally, we sorted R_{M1} and R_{M2} data sets separately with 2 M Ω intervals and plotted them against their respective occurrence frequencies to determine the pattern of frequency distributions. As shown in Figure 2c, the frequency distribution of the data sets between R_{M1} s and R_{M2} s matched almost perfectly ($n = 54$), which is consistent with the view that R_M can be reliably measured in dual patch recording.

Theoretically, R_M measurement is independent of R_a variation in dual patch recording. This was confirmed from the following experiments. First, in the correlation analysis shown in Figure 2d, R_M is not correlated with R_a . Second, the R_{a1} and R_{a2} measured from the same cell typically differ from each other, we next sorted out the large R_a ($R_{a,L}$) and small R_a ($R_{a,S}$) data sets into two groups from 10 dual patch recordings

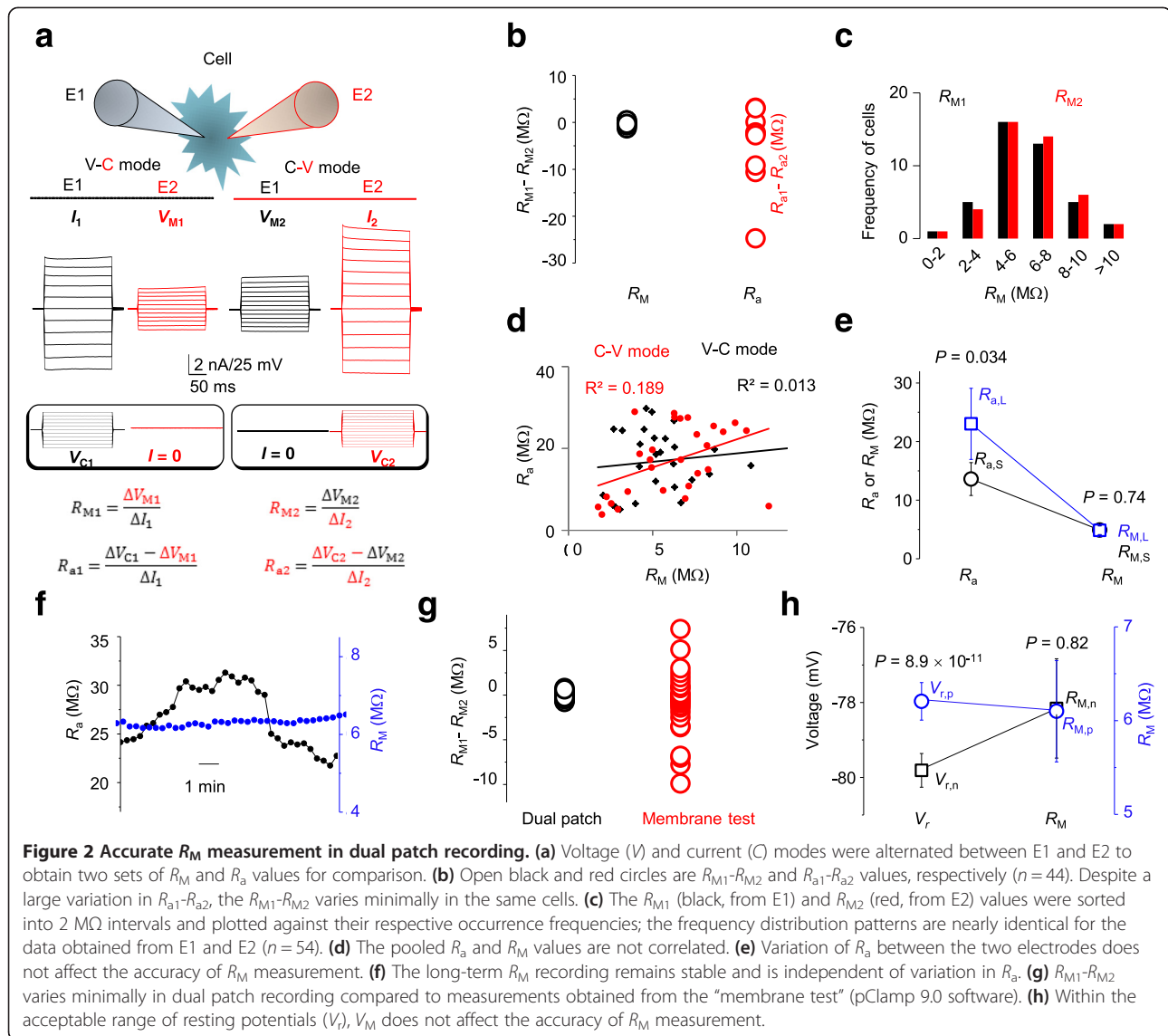


(Figure 2e). As anticipated, the $R_{a,L}$ and $R_{a,S}$ varied significantly ($R_{a,L}$, 23.02 ± 6.07 M Ω vs. $R_{a,S}$, 13.6 ± 2.8 M Ω , $n = 10$, $P = 0.034$), but their corresponding $R_{M,L}$ (4.85 ± 0.74 M Ω) and $R_{M,S}$ (4.90 ± 0.77 M Ω) were almost identical ($n = 10$, $P = 0.74$). Third, while the R_a varies considerably during long-term recording, the simultaneously measured R_M remained constant (Figure 2f).

In pClamp software, R_M can be measured from the “Membrane test” program, which has been widely used for study of astrocyte electrophysiology [5,8]. We found a much large variation between R_{M1} and R_{M2} data sets obtained from “Membrane test” than the data set from dual patch recording (Figure 2g), indicating that dual patch offers a more reliable and precise R_M measurement.

It should be noted that in single electrode recording, R_a is resolved from time constant (τ), i.e., $\tau = R_a C_M$. The accuracy of R_a estimation depends on a close approximation of

R_a to the effective access resistance ($R_{a,eff}$); that is $R_{a,eff} = R_a R_M / (R_a + R_M)$ [9]. In high R_M cells, such as neurons, $R_M \gg R_a$, so that $R_{a,eff} \cong R_a$, and R_a can be resolved with good confidence. However, in low R_M astrocytes, because $R_{a,eff} \cong R_M$, the R_a measured from “Membrane test” (pClamp9.0) is erroneous, so is R_M . The latter is calculated from $R_M = R_{total} - R_a$. Although we know that R_M in astrocyte is extremely low, but reliable R_M measurement is not yet available for the noted reason. Accordingly, our report provides a yet most reliable R_M measurement from mature astrocytes.

Within the acceptable whole-cell resting membrane potentials (V_r), i.e., more negative than -75 mV [10], the V_r values always vary slightly between E1 and E2 in the same cell. To ensure that within the accepted V_r range, variation of V_r does not affect R_M measurement, we sorted all the positive V_r ($V_{r,p}$) and negative V_r ($V_{r,n}$)

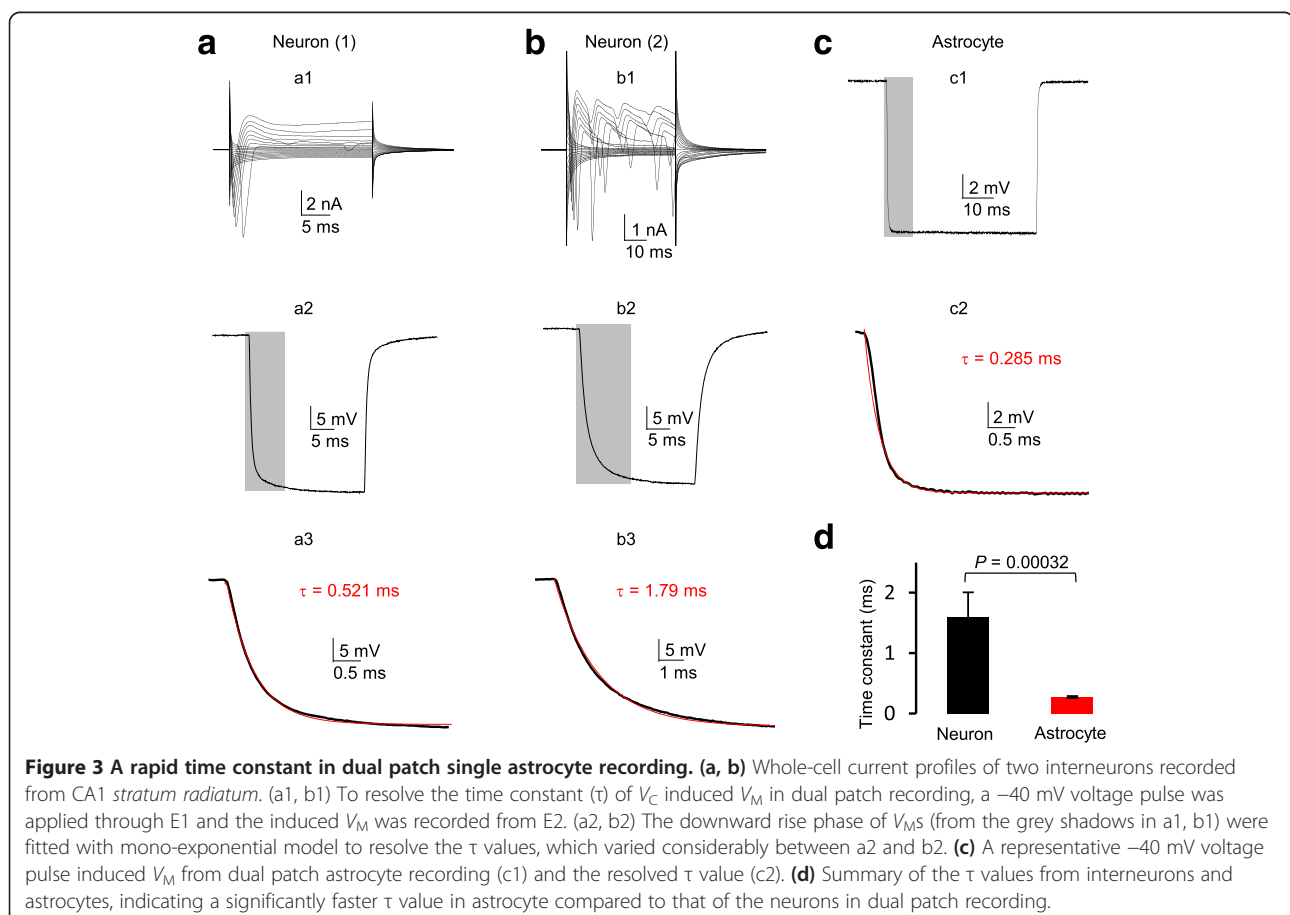
from 19 dual patch recordings into two separate groups for R_M comparison. While the $V_{r,p}$ (-77.97 ± 0.50 mV) and the $V_{r,n}$ (-79.81 ± 0.45 mV) varied significantly ($n = 19$, $P = 8.91 \times 10^{-11}$), the R_M was essentially the same between the two groups ($R_{M,p}$, 6.10 ± 0.54 M Ω vs. $R_{M,n}$, 6.13 ± 0.53 M Ω , $n = 19$, $P = 0.83$) (Figure 2h).

The experiments described above used young adult mice of 3–4 weeks old. To determine if this protocol is also applicable for astrocytes from fully mature mice brain, we next prepared slices from 5-month old mice. We found that dual patch single astrocyte recording remains feasible. At this animal age, dual patch recording revealed a similar V_r of -78.75 ± 0.47 mV ($n = 7$), and a R_M of 5.91 ± 1.52 M Ω ($n = 5$) compared to young adult mice.

In summary, we show that in dual patch recording, the R_M can be measured accurately and reliably, and the majority of astrocytes exhibit R_M values in the range of 4–8 M Ω . Importantly, since astrocytes are non-excitable, most of their ionic events can be monitored directly by R_M measurement. Thus, the ability of dual patch to permit long-term stable R_M measurement should be highly useful for pharmacological analysis of functional proteins in astrocytes, such as K^+ channels and transporters.

The temporal resolution in astrocyte dual patch recording

We next sought to answer how a compromised V_C affects the temporal resolution of the measured V_M from the E2, as poor temporal resolution hampers the ability of detecting ion channels with fast activation/inactivation kinetics. To address this, we dual patch recorded interneurons in CA1 *stratum radiatum* as control group for comparison of temporal resolution. Consistent with a previous report that hippocampal interneurons are morphologically and functionally diverse [8], the whole-cell current profile varied from cell to cell (Figure 3a, b). Nevertheless, interneurons do not express hyperpolarization-induced inward currents and showed a high R_M of 155 ± 41 Ω M ($n = 4$). Therefore, we applied a -40 mV voltage pulse through E1 to induce V_M change in E2. The time constant (τ) of V_M onset was used to analyze and compare the temporal resolution between neurons and astrocytes (Figure 3, a2, b2, c1), and τ was resolved from mono-exponential fit of the downward rise phase of V_M (Figure 3, a3, b3, c2). The τ varied from cell to cell in neurons with an average value of 1.60 ± 0.41 ms ($n = 4$). The τ varied much less among astrocytes (Figure 3c), 0.277 ± 0.015 ms ($n = 9$), which is significantly faster than that of interneurons.



Theoretically, a higher temporal resolution in astrocytes should also be attributable to the low R_M . Because τ is the product of effective access resistance ($R_{a,eff}$) times C_M , where $R_{a,eff} = R_a R_M / (R_a + R_M)$ [9]. As noted above, the $R_{a,eff}$ approximates to R_M in low R_M astrocytes, which results in a faster τ compared to high R_M neurons.

Because of an extremely high leak K^+ conductance, it is worth noting that the likelihood to observe a voltage dependent conductance in astrocyte whole-cell current depends chiefly on the expression quantity of the candidate channel, but not the temporal resolution of dual patch recording.

Experimental design

The following issues should be considered in the experimental design.

- (1) The advantage of using a combination of MultiClamp 700B (or 700A) amplifier and pClamp 9 (or 10) software is that the voltage and current clamp mode can be designated either the same or differently between E1 and E2. As the illustration shown in Figure 2a, E1 and E2 can be initially programmed in voltage (V) and current (C) clamp mode, respectively, and then swapped in the following experiment. For the electrode in V mode, the controlled input is V_C and the recorded signal is I . For the electrode in C mode with no holding current, the recorded signal is the V_M that is induced by V_C from another electrode in the pair. The voltage dependence and activation kinetics of ion channels of interest can then be constructed by plotting the measured I values against their corresponding V_M values (Figure 2a).
- (2) The measured V_M from E2 can be much smaller than that of the applied V_C in E1, which could make accurate V_M calculation difficult. When V_M cannot be detected with confidence, increase V_C to ensure a reliable V_M reading. Likewise, it is beneficial to set up one of the electrodes in the pair with a relatively small R_i in V mode.
- (3) The high leak K^+ conductance is the cause of difficulty for voltage clamp identification and pharmacological study of a specific K^+ channel of interest. The following examples will demonstrate how a combined pharmacology and current subtraction strategy can be used to overcome this obstacle in dual patch recording.
- (4) Channel inhibitors or activators are not yet available for most of two-pore channels, use of genetically modified mice, such as TWIK-1 and TREK-1 knockout mice, should be highly valuable to gain insights into the molecular identify and function of astrocyte passive conductance in the future [10].

- (5) The procedure described here should be equally useful for study of other cell type with similarly low R_M . When identification of ion channel with fast activation/inactivation kinetics is the purpose of study, a low R_a in both electrodes is essential and the commonly used conventions for single electrode recording also apply to dual patch recording.
- (6) When set up E1 and E2 in V and C mode, respectively, E2 only observes the deviation of V_M from the intended V_C . The measured V_M from E2 is not compensated for either dynamic or steady-state voltage errors. The former error is associated with the onset of a V_C and is proportional to the time constant ($\tau = R_a C_M$). The latter refers to the deviation of V_M from the steady-state holding V_C in response to rapidly activated ionic conductances, such as ionotropic GABA_A receptor in astrocytes (Figure 4). As noted above, effective R_a compensation cannot be reliably performed without the guidance of E2 as voltage monitor. Also, astrocytes show a faster V_M onset temporal resolution and unlikely express large amount of ion channels with rapid activation kinetics. Therefore, unless an experiment is designed to target on a specific voltage gated ionic conductance, R_a compensation is not recommended.
- (7) Other electrophysiological methods, such as discontinuous single electrode voltage clamp (dSEVC) and two electrode voltage clamp (TEVC) technique, typically use sharp electrode, which is technically unfeasible for mammalian astrocytes with a some diameter less than 10 μm . Additionally, no validated and commercially available amplifiers are yet available for the intended goal of present research. Therefore, at least in the current stage, these techniques cannot be considered as alternatives.

Advantages

Measurement of voltage-dependent membrane conductance: inwardly rectifying K^+ channels

Since V_M can be accurately measured in E2 when command voltages are applied through E1, the I - V relationship can be accurately established in low R_M astrocytes. To demonstrate this experimentally, we focused on the inwardly rectifying Kir4.1 K^+ channel, which expresses abundantly in astrocytes [11]. It has been shown in cultured astrocytes that 100 μM Ba^{2+} inhibits Kir4.1 currents fully and depolarizes V_M significantly [12]. In single electrode recording from astrocytes in slices, although 100 μM Ba^{2+} also depolarized membrane potential by 2.6 mV (-78.7 ± 1.1 mV in aCSF vs. -76.1 ± 1.0 mV in BaCl_2 , $P = 0.034$, $n = 7$, Figure 4a), the degree of V_M depolarization is much less than cultured astrocytes, and the overall passive conductance was not noticeably altered. The difficulty in

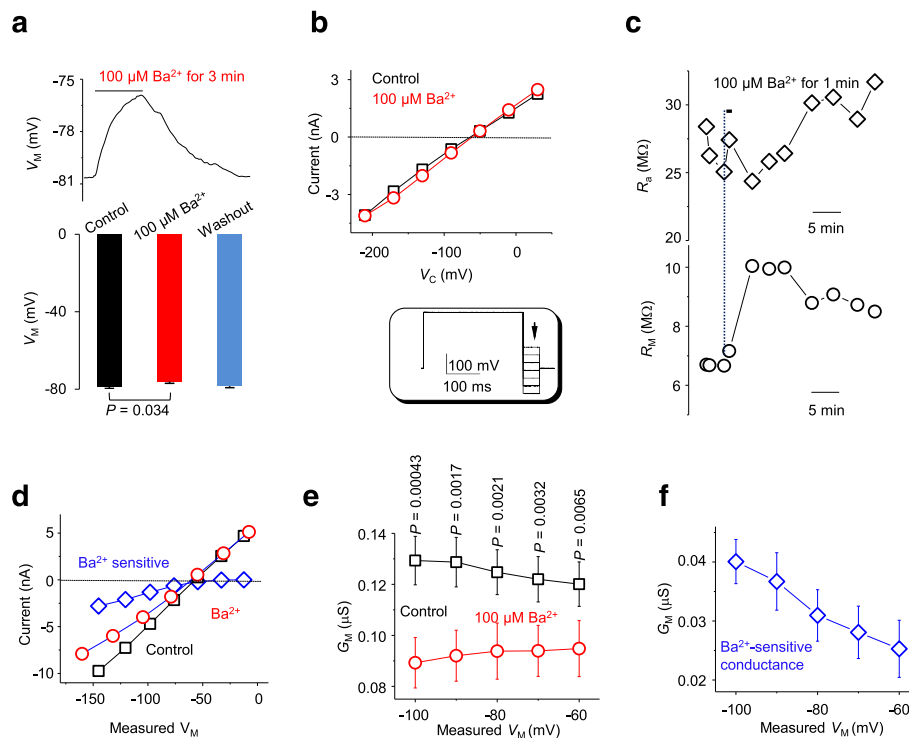


Figure 4 Disclosure of inwardly rectifying K⁺ conductance in dual patch recording. (a, b) Bath application of 100 μM Ba²⁺ produce a moderate V_M inhibition but not noticeable inhibition of inward currents using the conventional single electrode recording, although the V_M depolarizes by 2.6 mV with full recovery. Whole cell currents were induced by voltage steps from -210 to 30 mV with 30 mV increments. A pre-pulse voltage at 0 mV/300 ms was used to maximally activate Kir4.1 currents (inset). (c) Application of 100 μM BaCl₂ in dual patch induces a significant increase in R_M. (d) An example shows I-V_M relationships before (black) and after (red) 100 μM Ba²⁺ application. Ba²⁺ sensitive currents were resolved by subtraction of currents in the presence of Ba²⁺ application from the control. (e) A negative V_M-dependent G_M increase is inhibited totally by 100 μM Ba²⁺. Voltage dependent Ba²⁺ sensitive conductances are shown in (f).

resolving Kir4.1 currents with single electrode voltage clamp recording is shown in Figure 4b. To maximally activate Kir4.1 currents, a 300 ms pre-pulse to 0 mV was used prior to the stepwise command voltages (inset, Figure 4b) [12]. These yielded no indication of inward rectification of whole-cell currents. In addition to a complex expression of other K⁺ channels that obscure the activation kinetics of Kir4.1 in astrocytes [11], poor voltage clamp quality be majorly is likely responsible for this.

In dual patch R_M measurement, one minute 100 μM Ba²⁺ bath application increased R_M from the control 7.46 ± 1.2 MΩ to 13.7 ± 3.1 MΩ (n = 7), corresponding to a membrane conductance (G_M) decrease from 0.134 μS in the control to 0.073 μS in the Ba²⁺. Based on this analysis, Kir4.1 accounts for ~45.5% of the G_M (Figure 4c).

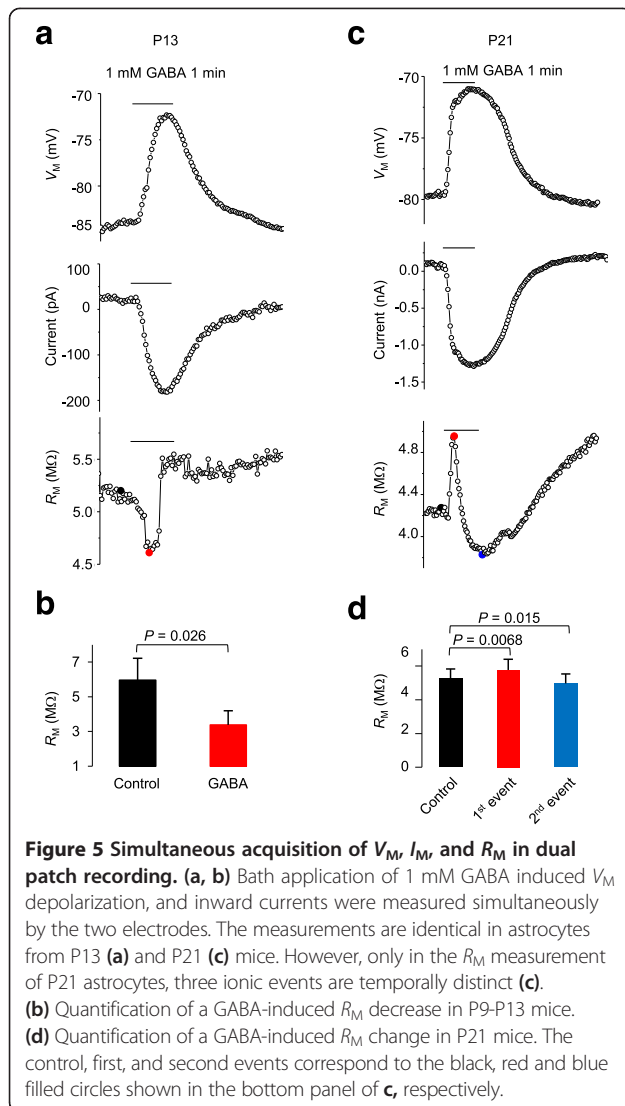
As the V_C-induced actual V_M can be reliably determined to construct the actual I-V_M relationship for a conductance of interest, we next adjusted the V_C to reach the intended V_M from -60 mV to -100 mV, where the inward rectification kinetics of Kir4.1 should be evident [12]. The I-V_M curves shown in Figure 4d revealed a selective inhibition of inward whole-cell currents by Ba²⁺. To analyze the results statistically, we used voltage

dependent G_M to describe the rectification characteristics. We show that a voltage-dependent inward G_M was clearly evident in the control condition (Figure 4e-f), which is consistent with the presence of functional Kir4.1 currents. Furthermore, this inwardly rectifying conductance was totally inhibited by 100 μM Ba²⁺. These results demonstrate that dual patch allows reliable establishment of I-V_M relationship and, in the present case, enables the functional identification and pharmacological analysis of inwardly rectifying Kir4.1 channels in astrocytes.

Identification of multiple ionic events associated with GABA_A receptor activation

A unique technical advantage of dual patch recording is that I, V_M and R_M can be measured and resolved simultaneously. We chose the astrocytic GABA_A receptor as an example to experimentally demonstrate the feasibility of this powerful application.

We have recently shown that, while GABA_A activation decreases R_t in both neurons and NG2 glia, GABA_A activation increases R_t in astrocytes, which is likely caused by a rapid secondary K⁺ channel inhibition [13].



However, single electrode recording in either voltage or current clamp mode does not provide a temporal resolution to separate these ionic events in astrocytes. Therefore, we further explored this issue in dual patch recording, where GABA-induced changes in V_M , I and R_M can be obtained simultaneously. Interestingly, astrocytes at different developmental stages responded to GABA differently. At P13, immature astrocytes responded to 1 mM GABA application by V_M depolarization, activation of inward currents and R_M decrease (5.96 ± 1.26 M Ω in control vs. 3.37 ± 0.82 M Ω in GABA, $n = 5$, $P = 0.026$) (Figure 5a-b), responses which were identical to neuronal GABA_A receptor activation [13]. By comparison, in mature P21 astrocytes, while 1 mM GABA also induced inward currents and V_M depolarization, three obvious ionic events could be resolved in R_M measurements (Figure 5c-d). Specifically, the R_M first increased from the control 5.27 ± 0.56 M Ω to 5.77 ± 0.63 M Ω ($n = 6$,

$P = 0.0068$), then decreased significantly (4.97 ± 0.57 M Ω , $n = 6$, $P = 0.015$). This effect was followed by a second sustained R_M increase, implying a complex modulation of astrocyte membrane conductance upon GABA_A activation.

As noted above, simultaneous measurement of I , V_M and R_M is feasible in dual patch recording. Additionally, only in this recording mode, multiple ionic events associated with astrocytic ionotropic GABA_A receptor activation could be readily identified. This powerful application should also be applicable for revealing complex ionic events in other cell types, such as neurons.

Summary of technical advantage of dual patch single astrocyte recording

1. As noted before, the R_a and R_M measurement from single electrode "Membrane test" software program are erroneous; this protocol allows accurate, stable and long-term R_M measurement from astrocytes. For non-excitable cells, this should have a broad usage for reliable pharmacological analysis of ion channel and electrogenic transporter activity in astrocytes.
2. An important purpose of this protocol is to validate whether the voltage dependence of a specific ionic conductance can be established and analyzed. We show from the G_M analysis of Kir4.1 currents that this is feasible (Figure 4).
3. A unique advantage we demonstrated in this protocol is that membrane I , V_M , and R_M can be measured simultaneously in dual patch recording model. As shown in the example of astrocytic GABA_A receptor study, multiple ionic events can be disclosed following to GABA_A receptor activation (Figure 5).
4. Although it may not be highly useful, using E2 as a monitor, it is possible to achieve a nearly perfect voltage clamp quality with R_a compensation function (Figure 1h). This can not be done in single electrode voltage clamp recording.

Potential limitation

The voltage clamp method is designed to reveal the voltage dependence of membrane conductances. Using Kir4.1 channel currents as an example (Figure 4), we demonstrated that the voltage dependence can be accurately established and pharmacologically analyzed in dual patch recording. However, even though the temporal resolution of V_M onset is faster in astrocytes (Figure 3), identification of low density expressing voltage-dependent ion channel conductance in low R_M astrocytes remains challenging. For example, immature astrocytes express voltage- and time-dependent outward transient K⁺ channels [3], but whether the expression of these channels continues in

mature astrocytes cannot be answered with confidence with dual patch recording. Nevertheless, there is no evidence indicating extensive expression of voltage gated ion channels in astrocytes [11].

It is worth noting that two recent reports have successfully used dual patch single astrocyte recording to correct voltage error for analyzing the relative glutamate vs. Cl^- permeability ratio through Best1 channel [14], and identifying pH sensitive and anesthetic-sensitive leak K conductances in hippocampal astrocytes [15]. Thus, the dual patch method validated in this study provides a powerful means for studying the voltage dependence of leak type K^+ channels, slow cycling transporters, and pumps that are abundantly expressed in astrocytes.

Materials

Reagents

- CaCl_2 , glucose, HEPES, KCl, KOH, Mg-ATP, MgCl_2 , $\text{Na}_2\text{-GTP}$, NaCl, NaHCO_3 , NaH_2PO_4 (all from Sigma-Aldrich, St. Louis, MO)
- Sulforhodamine 101 (SR101) from Invitrogen (New York, NY)
- Deionized water with $18.2 \text{ M}\Omega\cdot\text{cm}$ at 25°C
▲ CRITICAL The quality of water is especially important for internal solutions.
- C57BL/6 J mice from postnatal day (P) 9–30, and 5 months old were used in different experiments noted. ! CAUTION All animal studies must be approved by the Institutional Animal Care and Use Committee. All the relevant ethics regulations have to be strictly followed. ▲ CRITICAL The animal age needs to be carefully chosen depending on experimental purpose and we chose to use animals older than postnatal day 21 in most of the experiments as hippocampal astrocytes become mature after this postnatal day. To validate this protocol for study astrocytes from fully mature mice, 5-month old mice were used in some of experiments.

Equipment

- An electrophysiology setup for submerged slices equipped with $\times 4$ and $\times 40$ infrared differential interference contrast (IR-DIC) visualization, a patch-clamp amplifier capable of current and voltage clamp and providing two channel recording (e.g., MultiClamp 700A or 700B, Molecular Devices), an interface for converting digital-analog signals between the amplifier and a computer (e.g., Digidata 1322A, Molecular Devices).
- (Optional) A fluorescent imaging system (e.g., Polychrome V system from Till Photonics, Germany) is advantageous for high resolution

visualization of small glial soma and placing of dual patch electrodes on it. This system can also be used for identifying astrocyte based on SR101 positive staining. This system can also be used for simultaneous dual patch and ion sensitive dye measurement.

- Two micromanipulators for automatic loading of two electrodes to the top of the brain slice can shorten the loading time (e.g., PatchStar from Scientifica, UK).
- Commercially available borosilicate glass capillaries, such as the one from Warner Instruments (Cat. no. 64–0772), worked well in this experiment. An open electrode resistance in the range of $2.5\text{-}5 \text{ M}\Omega$, when filled with KCl-based electrode solution, is well suited for dual patch recordings. However, for low R_M astrocytes, electrode resistance in the low-end of this range is recommended.

Reagent setup

Brain slice cutting solution (in mM): 125 NaCl, 3.5 KCl, 25 NaHCO_3 , 1.25 NaH_2PO_4 , 0.1 CaCl_2 , 3 MgCl_2 , and 10 glucose. Cutting solution should be freshly prepared on the day of the experiment.

Artificial cerebral spinal fluid (aCSF) (in mM): 125 NaCl, 3.5 KCl, 25 NaHCO_3 , 1.25 NaH_2PO_4 , 2 CaCl_2 , 1 MgCl_2 , and 10 glucose (osmolality, $295 \pm 5 \text{ mOsm}$) at room temperature ($20\text{-}22^\circ\text{C}$).

Electrode solution (in mM): 140 KCl, 0.5 CaCl_2 , 1 MgCl_2 , 5 EDTA, 10 HEPES, 3 $\text{Mg}^{2+}\text{-ATP}$, and 0.3 $2\text{Na}^+\text{-GTP}$. This solution was titrated with KOH to pH 7.25–7.27, and the final osmolality was $280.0 \pm 5.0 \text{ mOsm}$. The solution can be prepared in advance and stored at -80°C in $\sim 0.5 \text{ ml}$ aliquots.

SR101: Stock solution, 6 mM; working solution, 0.6 μM .

Procedure

1 | Use a commercially available Vibratome, e.g., Pelco 1500, to prepare 250 μm thickness coronal hippocampal slices from mouse brain with a standard procedure we and others described before [5,16]. All solutions should be continuously bubbled with $95\% \text{O}_2/5\% \text{CO}_2$.

2 | Place acute slices in a nylon net basket slice holder immersed in aCSF chamber for recovery and storage. The aCSF is continuously bubbled with $95\% \text{O}_2/5\% \text{CO}_2$ for a typical experiment day of 6 to 8 hrs.

3 | For SR101 staining, transfer slice containing basket to another aCSF chamber containing 0.6 μM SR101 at 34°C for 30 min. Then, transfer the same basket back to the normal aCSF at room temperature for at least 1 h before experiment.

4 | For recording, transfer one brain slice to the recording chamber, lay it down on the bottom of glass chamber and gently place a platinum slice anchor (Warner Instruments) on the top of slice to prevent

movement of slice from bath perfusion. Perfuse oxygenated aCSF at a rate of 2.5 ml/min.

5 | Fill two patch electrodes with electrode solution and install them to the electrode holders. Apply a small and constant positive pressure to the internal solution. Use IR-DIC with $\times 4$ objective to identify the surface of the slice. Move the tips of electrodes to the region of interest, i.e., CA1 *stratum radiatum*. In voltage clamp mode, apply a recurrent 5 mV square voltage pulse to monitor the electrode resistance. Switch to the water immersion $\times 40$ objective. Apply a drop of bath solution to the objective that runs down and forms a fluid bridge between the front lens and the slice. Advance electrodes into the slice ~ 50 μm beneath the surface.

6 | Select a viable glial cell based on an irregular soma shape with a diameter around 10 μm . Typically, one or more primary processes stemming from the soma are visible (Figure 1a). To confirm an astrocytic identify, SR101 staining can be used. However, be aware that an adverse effect on neuronal excitability has been reported with SR101 staining [17]. After establishing the whole-cell configuration, mature astrocytes can be unequivocally identified by the expression of passive conductance (Figure 1b). Alternatively, astrocytes can be identified solely and easily by SR101 staining. Switch to IR-DIC visualization.

7 | Approach the cell slowly with one electrode at a time. Once on-cell, see dimpling and release the electrode pressure. Apply negative potential (ranging from -70 to -80 mV) through the commander panel to facilitate seal formation. This manipulation typically results in the rapid formation of a $G\Omega$ seal. Repeat this procedure with the second electrode. Check and keep the position of first electrode relative to the cell. Finally, ensure both electrodes to form $G\Omega$ seal on the same cell.

▲ CRITICAL This is the most critical step requiring careful coordination of two electrodes and readjustment of the relative position between cell soma and electrodes. Often, when the targeted cell is approached by the second electrode, the cell can move away from the first electrode. Adjust the first electrode to follow the cell when it is necessary.

? TROUBLESHOOTING(1)

8 | Rupture the patch of membrane isolated inside the electrode tip by negative pressure pulses to establish the whole-cell configurations. No obvious change in holding current shift associated with a decrease of seal test resistance to < 30 M Ω is an indication of successful formation of whole-cell configuration. Repeat this for the second electrode. After both whole-cell configurations are established, wait at least 5 min to allow ion equilibration between electrode solution and intracellular cytoplasm

? TROUBLESHOOTING(2)

9 | Set astrocyte in desired mode, e.g., with one electrode in current clamp and another electrode in voltage

mode under the control of Clampex 9.2. Program both channels in either voltage or current clamp mode depending on experimental purpose.

- (a) To evaluate the voltage dependence of channel activation, apply a series of command voltage steps, e.g., -210 mV to $+30$ mV in 40 mV increments, from the holding potential of -80 mV
- (b) To monitor change of R_M (or R_t) in response to drugs, e.g., GABA, apply a single negative command voltage step, e.g., -60 mV from holding potential for 20 ms.

? TROUBLESHOOTING(3)

10 | Analyze dual patch results.

- (a) $I-V_M$ relationship can be derived from the stepwise command voltages as shown in Figure 2a. Plot I readings from E1 against their corresponding V_M readings from electrode 2. Determine the reversal potential of the current by extrapolating the data point on the $I-V_M$ curve.
- (b) Plot the conductance-voltage ($G-V_M$) curve by dividing the current amplitude change (ΔI) by the measured voltage step (ΔV_M) at each potential. As shown in Figure 4f.

? TROUBLESHOOTING

Step 7, when $G\Omega$ is difficult to establish, check the following possibilities:

- a) Brain slice quality is always the first thing to be considered. Ensure the preparation procedure was followed strictly; otherwise a new preparation is needed.
- b) The difficulty in achieving $G\Omega$ seal increases with animal age, start your practice with P10 mice is recommended to familiarize the procedure. Young adult mice from P21 - P30 can be used in most of experiments, unless the study targets on an age related subject.
- c) Make sure to apply and maintain a small positive pressure before the electrodes touching to the bath solution in step 5.
- d) Apply the suction as gentle as possible and increase it in a stepwise manner until the membrane is ruptured.
- e) Ensure electrode solution is freshly prepared with correct pH and osmolality.

If the seal in the first electrode is lost when the second electrode approaches the cell, pay attentions to the following:

- a) Focus on the cell when the second electrode approaches the cell. Move the first electrode to follow the cell if the cell moves.

- b) Adjust slice anchor and hold more tightly if too loose.
- c) The deeper the targeted cell beneath the surface of slice, the more likely to encounter a cell movement during the handling the second electrode to approach the cell. Select a relatively shallow cell, ~50 μm is recommended.
- d) Approach the cell gently. Avoid larger movements of the second electrode, including approaching, going up or down. If the tip of the second electrode is too shallower or deeper than cell body, withdraw the second electrode gently, adjust the position on the top of slice and re-approach.

Step 8, apply suction pulses either by mouth or use of a syringe. Try following options:

- a) In our experience, a relatively strong and fast pulse works well to rupture membrane and achieve a relatively stable R_a .
- b) Keep the same or increase the suction pressures in the repetitive rupture attempt, release pressure immediately if membrane resistance in seal test drops suddenly.
- c) Keep a small pressure and click “Zap”, and release the pressure after Zap. Repeat Zap if necessary.
- d) If the seal resistance is higher than 30 $\text{M}\Omega$, indication of $R_t > 30 \text{M}\Omega$, repeat above steps may decrease the R_t of whole-cell recording.

Step 9, R_a tends to increase during recording (Figure 2f), do the following to minimize it:

- a) Low resistance electrodes, i.e., 2.0-2.5 $\text{M}\Omega$, has been demonstrated to be feasible and is recommended [18]; as such, the R_t can be physically reduced to the lowest workable range.
- b) Empirically, a relatively stronger suction pressure for whole-cell break-through results in a high percentage of low and stable R_a whole-cell recordings.
- c) To ensure that the brain slice is anchored securely in the chamber; this prevents potential slice movement resulting from perfusion pulsatile.
- d) In general, the older the animal the more difficulty to achieve a long-lasting stable R_a , use young adult animals unless the experiment examining an ageing related question.
- e) Use mechanically stable micromanipulators.
- f) We routinely discard recordings with high R_a (or R_t) from data analysis.

•Timing

Step 1, slice preparation: 30 min

Step 2–3, slice recovery and SR101 staining: at least 1 h

Step 4, transfer slice to recording chamber and re-equilibration: 20 min

Step 5, loading both electrodes: 10 min

Step 6, select astrocyte: 5 min

Step 7, approach the cell and form $\text{G}\Omega$ seals: 5–30 min

Step 8, break through to form dual patch recording: 3–10 min

Step 9, recording: 30 min - 4 h, depending on the experimental design

Step 10, Analysis: variable, depending on required data.

Anticipated results

Dual patch recording was once considered to be a time-consuming technique which required considerable skill. Facilitated by the use of advanced equipment, specifically PatchStar micromanipulators and software (Scientifica, UK), a Polychrome V imaging system (Till Photonics, Germany), and a MultiClamp 700A/700B amplifier (Molecular Devices, Sunnyvale, CA), this recording mode can be performed routinely, studying 3–8 cells in a 6-hour experimental day. For experienced researcher, the dual patch single astrocyte recording can be achieved within 10 min after the cell being visual identified. Should all the steps be followed carefully, successful dual patch single astrocyte recording can be readily achieved. In some of the experiments, successful dual patch recordings recording had lasted up to 4 hours in our designed experiment. Thus, dual patch is an ideal technique for the future study of functional channels, receptors, and electrogenic transporters in astrocytes.

Competing interests

The authors declare that they have no competing interests.

Authors' contributions

BM and MZ conceived the study. All the authors were involved in the design of the experiments and discussion of the results. BM and GX performed experiments and analyzed the data. BM, GX, JJE, and MZ wrote the manuscript. MZ supervised the research. All authors read and approved the final manuscript.

Acknowledgments

This work was sponsored by grants from the National Institute of Neurological Disorders and Stroke (RO1NS062784 to MZ) and the National Natural Science Foundation of China (81000491 to GX). We thank Ms. Judith A. Eneyart and Ms. Kelly E. Crowe for their assistance in manuscript preparation, Mr. Randall Carpenter for critical reading of manuscript.

Author details

¹Department of Neuroscience, The Ohio State University Wexner Medical Center, Columbus, OH 43210, USA. ²Department of Neurology, Tongji Hospital, Tongji Medical College, Huazhong University of Science and Technology, Wuhan 430030, P.R. China.

Received: 27 January 2014 Accepted: 13 March 2014

Published: 17 March 2014

References

1. Berger T, Schnitzer J, Kettenmann H: Developmental changes in the membrane current pattern, K⁺ buffer capacity, and morphology of glial cells in the corpus callosum slice. *J Neurosci* 1991, **11**:3008–3024.

2. Steinhäuser C, Berger T, Frotscher M, Kettenmann H: **Heterogeneity in the Membrane Current Pattern of Identified Glial Cells in the Hippocampal Slice.** *Eur J Neurosci* 1992, **4**:472–484.
3. Zhou M, Schools GP, Kimelberg HK: **Development of GLAST(+) astrocytes and NG2(+) glia in rat hippocampus CA1: mature astrocytes are electrophysiologically passive.** *J Neurophysiol* 2006, **95**:134–143.
4. Kafitz KW, Meier SD, Stephan J, Rose CR: **Developmental profile and properties of sulforhodamine 101–Labeled glial cells in acute brain slices of rat hippocampus.** *J Neurosci Methods* 2008, **169**:84–92.
5. Zhou M, Xu G, Xie M, Zhang X, Schools GP, Ma L, Kimelberg HK, Chen H: **TWIK-1 and TREK-1 are potassium channels contributing significantly to astrocyte passive conductance in rat hippocampal slices.** *J Neurosci* 2009, **29**:8551–8564.
6. Hille B: *Ion channels of excitable cells.* Sunderland, MA: Sinauer; 2001.
7. Xie M, Lynch DT, Schools GP, Feustel PJ, Kimelberg HK, Zhou M: **Sodium channel currents in rat hippocampal NG2 glia: characterization and contribution to resting membrane potential.** *Neuroscience* 2007, **150**:853–862.
8. Djukic B, Casper KB, Philpot BD, Chin LS, McCarthy KD: **Conditional knock-out of Kir4.1 leads to glial membrane depolarization, inhibition of potassium and glutamate uptake, and enhanced short-term synaptic potentiation.** *J Neurosci* 2007, **27**:11354–11365.
9. Lindsay R, Caroline J, Winter J: *Molecular Neurobiology.* Oxford: Oxford University Press; 1991.
10. Wang W, Putra A, Schools GP, Ma B, Chen H, Kaczmarek LK, Barhanin J, Lesage F, Zhou M: **The contribution of TWIK-1 channels to astrocyte K(+) current is limited by retention in intracellular compartments.** *Front Cell Neurosci* 2013, **7**:246.
11. Cahoy JD, Emery B, Kaushal A, Foo LC, Zamanian JL, Christopherson KS, Xing Y, Lubischer JL, Krieg PA, Krupenko SA, Thompson WJ, Barres BA: **A transcriptome database for astrocytes, neurons, and oligodendrocytes: a new resource for understanding brain development and function.** *J Neurosci* 2008, **28**:264–278.
12. Ransom CB, Sontheimer H: **Biophysical and pharmacological characterization of inwardly rectifying K⁺ currents in rat spinal cord astrocytes.** *J Neurophysiol* 1995, **73**:333–346.
13. Ma BF, Xie MJ, Zhou M: **Bicarbonate efflux via GABA(A) receptors depolarizes membrane potential and inhibits two-pore domain potassium channels of astrocytes in rat hippocampal slices.** *Glia* 2012, **60**:1761–1772.
14. Park H, Han KS, Oh SJ, Jo S, Woo J, Yoon BE, Lee CJ: **High glutamate permeability and distal localization of Best1 channel in CA1 hippocampal astrocyte.** *Mol Brain* 2013, **6**:54.
15. Chu KC, Chiu CD, Hsu TT, Hsieh YM, Huang YY, Lien CC: **Functional identification of an outwardly rectifying pH- and anesthetic-sensitive leak K(+) conductance in hippocampal astrocytes.** *Eur J Neurosci* 2010, **32**:725–735.
16. Debanne D, Boudkkazi S, Campanac E, Cudmore RH, Giraud P, Fronzaroli-Molinieres L, Carlier E, Caillard O: **Paired-recordings from synaptically coupled cortical and hippocampal neurons in acute and cultured brain slices.** *Nat Protoc* 2008, **3**:1559–1568.
17. Kang J, Kang N, Yu Y, Zhang J, Petersen N, Tian GF, Nedergaard M: **Sulforhodamine 101 induces long-term potentiation of intrinsic excitability and synaptic efficacy in hippocampal CA1 pyramidal neurons.** *Neuroscience* 2010, **169**:1601–1609.
18. Xu G, Wang W, Kimelberg HK, Zhou M: **Electrical coupling of astrocytes in rat hippocampal slices under physiological and simulated ischemic conditions.** *Glia* 2010, **58**:481–493.

doi:10.1186/1756-6606-7-18

Cite this article as: Ma et al.: Dual patch voltage clamp study of low membrane resistance astrocytes *in situ*. *Molecular Brain* 2014 **7**:18.

Submit your next manuscript to BioMed Central and take full advantage of:

- Convenient online submission
- Thorough peer review
- No space constraints or color figure charges
- Immediate publication on acceptance
- Inclusion in PubMed, CAS, Scopus and Google Scholar
- Research which is freely available for redistribution

Submit your manuscript at
www.biomedcentral.com/submit

